Premelting disordering of the Si(113) surface studied by tight-binding molecular dynamics

1996 J. Phys.: Condens. Matter 8 6511

(http://iopscience.iop.org/0953-8984/8/36/004)

J. Phys.: Condens. Matter **8** (1996) 6511–6523. Printed in the UK

Premelting disordering of the Si(113) surface studied by tight-binding molecular dynamics

T H Wee, Y P Feng†, C K Ong and H C Poon

Department of Physics, National University of Singapore, Singapore 119260, Singapore

Received 27 February 1996, in final form 9 May 1996

Abstract. The tight-binding molecular-dynamics method is used to study melting of the 3×1 reconstructed Si(113) surface. It is found that the surface starts to disorder at about 950 K which is consistent with recent low-energy-electron-diffraction and x-ray chiral melting studies. The behaviour of the simulated mean square atomic displacement and static structure factor indicate that the surface disorders anisotropically. A surface quasi-liquid which exhibits properties of both crystalline and liquid phase is observed between 1000 K and 1400 K. Surface-initiated melting of the crystal is expected to take place at a temperature slightly above 1400 K but lower than the bulk melting temperature.

1. Introduction

Investigation of semiconductor high-Miller-index surfaces are rare because these surfaces are generally unstable. They tend to facet into lower-index planes upon annealing. However, the Si(113) surface constitutes an interesting exception. Besides thermodynamically stable, the bulk-truncated Si(113) surface contains one twofold-coordinated atom and one threefold-coordinated atom, so that on Si(113) local bonding configurations of Si(111) and Si(001) are combined. This makes this surface interesting for heteroepitaxy.

Because of these properties, the Si(113) surface has received much attention [1–25]. Most of these studies have been on the reconstructions of the surface near room temperature. Even though the atomic structure of the Si(113) surface is not yet completely solved, the majority of theoretical and experimental studies have found that the Si(113) surface reconstructs to a 3×2 structure [2–16] at room temperature, which may transform into a 3×1 structure in the presence of residual gases [10, 11] or at high temperature [14–16]. Xing *et al* [14] studied the atomic structure of the Si(113) surface at high temperature ($>$893 K) using low-energy electron diffraction (LEED). They observed a LEED pattern corresponding to the 1×1 unreconstructed surface structure at 923 K. When the specimen was cooled below 873 K, the 1×1 structure started to be replaced by a 3×1 superstructure, which held until about 723 K. At this temperature, the phase transition from 3×1 to 3×2 is observed. When the specimen temperature fell below 673 K, the surface finally reconstructed to the 3×2 structure, which remained until room temperature. Raising the specimen temperature again, LEED patterns indicate that the order–order phase transitions on the Si(113) surface are reversible. Our computer simulation study [15] using a tight-binding molecular dynamics (TBMD) method has confirmed this order–order phase transition.

† Author to whom correspondence should be addressed

0953-8984/96/366511+13$19.50

Due to interest in understanding two-dimensional (2D) phase transition, the order–disorder phase transition of the 3×1 reconstructed Si(113) surface has been studied [16–19]. This surface has been used as a prototype material in demonstrating chiral melting which is a continuous two-dimensional phase transition directly from a commensurate solid into an incommensurate fluid. Here, the reconstructed surface layer plays the role of the 2D system which undergoes phase transformations. The unreconstructed deeper layers may be considered as the substrate supplying adsorption sites. Yang *et al* [19] have presented a spot-profile-analysis low-energy-electron-diffraction (SPA-LEED) study of the disordering of the Si(113) 3×1 reconstruction. They have observed an asymmetric broadening and a shift away from the commensurate position for the 3×1 LEED spot. They argued that their findings on various critical exponents and the temperature dependence of the incommensurability are consistent with chiral melting. Schreiner *et al* [16] have studied the 3×1 order–disorder phase transition of the Si(113) and Ge(113) surfaces using SPA-LEED. They have found that the Si(113) 3×2 surface experiences a transition into a 3×1 reconstructed surface which is completed at about 780 K. At $T_c \approx 929$ K the silicon undergoes an order–disorder phase transition from 3×1 into a 1×1 disordered surface. Close to the order–disorder transition temperature (T_c) the 3×1 LEED spot intensities drop down to zero. Above T_c the 3×1 superlattice spots broaden and continuously move away from the commensurate position. The characteristics of the transitions are compared to chiral melting. It turned out that the experiments for Ge(113) give more convincing evidence for chiral melting with isotropic scaling than those for Si(113). Abernathy *et al* [17, 18] reported x-ray-scattering studies of the (3×1)–disordered phase transformation of the Si(113) surface. A continuous commensurate-solid–incommensurate-fluid transformation at $T_c = 950\pm40$ K was observed. At the transformation, the reconstructed layer becomes uniaxially incommensurate along the cubic $(1\bar{1}0)$ direction. It remains commensurate along the $(33\bar{2})$ direction. The observed critical behaviour is consistent with the prediction for chiral melting.

However, to our knowledge, the behaviour of the Si(113) surface at higher temperature has not been studied. Being interested in the behaviour of the surface structure at higher temperature and how it eventually leads to melting of the underlying crystal, we have performed a tight-binding molecular dynamics simulation study on the melting of the Si(113) surface. It is found that the 3×1 reconstructed Si(113) surface starts to disorder at about 950 K, which coincides with experimental observation. Furthermore, we found that the surface disorders anisotropically. A surface-initiated melting of the crystal is predicted to occur at temperatures above 1400 K but below the bulk melting temperature.

2. Computational details

In this study, we employ the parametrized tight-binding molecular dynamics method which has been proven to be one of the most useful theoretical tools in probing the microscopic properties of semiconductors [26–29]. Although this method is less rigorous than the local-density-functional approximation (LDA) method, its main advantage is its ability to handle a large number of atoms. Therefore, a more realistic system can be modelled and studied, especially when studying higher-order reconstruction of the Si surface [15, 30–32]. The details of the tight-binding molecular-dynamics method used in this study can be found in [26] and [30]. We incorporated the molecular-dynamics (MD) techniques into the tight-binding (TB) total-energy scheme for Si, following the prescription of Khan and Broughton [26]. The total-energy expression due to Tománek and Schlüter [33] was modified to include a smooth cutoff function so as to facilitate MD simulation. We also adopt their scheme of constructing a fictitious Lagrangian to simulate the physical trajectories of the nuclei while

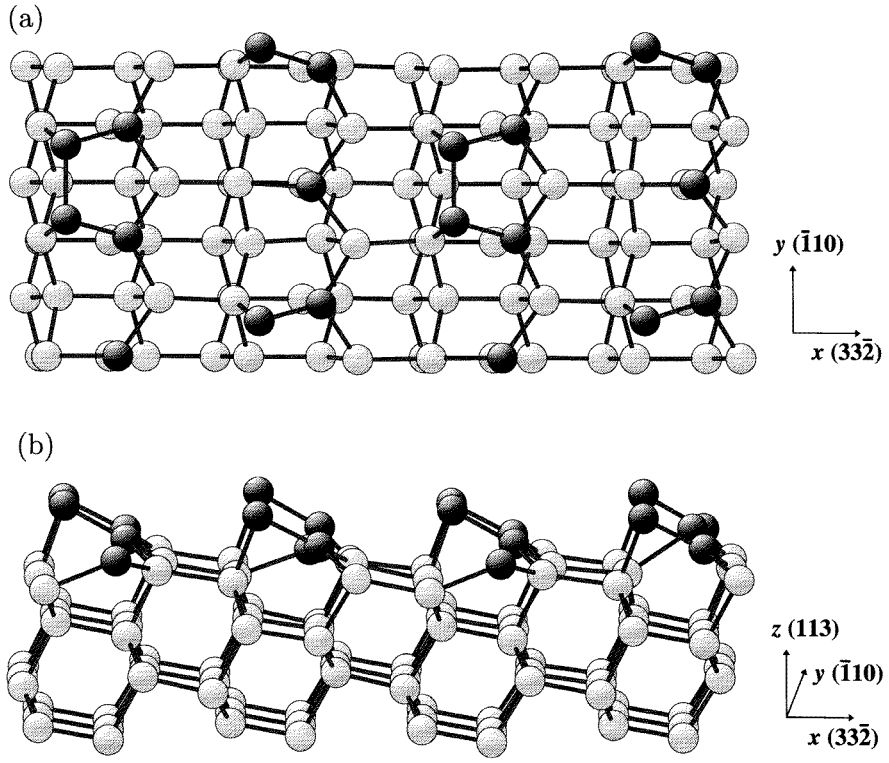

Figure 1. (a) Top and (b) side view of the simulation cell.

keeping the electrons close to their quantum ground state.

We begin our simulation from the fully relaxed 3×1 surface structure (figure 1) which we have obtained using the TBMD method [15]. The simulation cell consists of a slab of five layers of Si atoms. Each layer contains 24 atoms except the top layer which forms the 3×1 reconstructed surface containing 20 atoms. For the convenience of the following discussion, we choose a coordinate system whose x- y- and z-axes are along the $(33\bar{2})$, $(\bar{1}10)$ and (113) directions respectively, as shown in figure 1. In addition, a layer of 'H' atoms, which is not shown in figure 1, is used to saturate the lowest layer of Si atoms. These 'H' atoms are meant to minic Si atoms in the bulk and their parameters in the total-energy expression for the slab are chosen to simulate Si atoms. Periodic boundary conditions are applied in the plane of the surface to simulate a surface extending to infinity.

During the simulations, the Si atoms in the top four layers are allowed to move and interact with neighbouring atoms while the atoms in the two bottom layers (Si and 'H' atoms in the fifth and sixth layers, respectively) are kept fixed but are allowed to change their electronic structures as a result of interaction with neighbouring atoms. The TB band structure calculations are performed at the Γ-point within the Brillouin zone, which is justified since the real-space computational cell used in our calculation is much larger than the primitive unit cell of Si and the Brillouin zone is therefore very small. For finite-temperature simulation, the electrons are still kept in their ground state by invoking the Born–Oppenheimer theorem. This means that at all times, for a given instantaneous

position of the ions, the total energy expression is kept at a minimum with respect to the electronic coordinates, subject to the orthonormality constraints of the wave functions. This minimization has been referred as quenching of the electrons to the Born–Oppenheimer surface. After each quenching, the trajectories of both the ionic and electronic coordinates are updated simultaneously with the Verlet algorithm. This is repeated for 100 time steps (each time step corresponds to 1.08×10^{-16} s) after which the electrons are quenched to the Born–Oppenheimer surface again and the procedure is repeated. During the 100 steps, a 'Shake' algorithm [34] is used to impose the orthonormality constraints in the updating of the electronic coordinates.

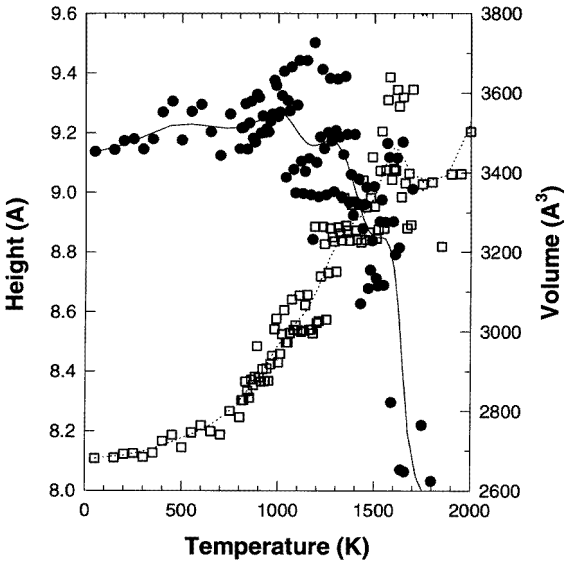

Figure 2. Thickness (●) and volume (□) of the simulation cell are shown as functions of temperature. The lines are Bazier curves fitted to the data points.

For temperatures below 700 K, the surface structure changes slowly as the temperature is increased and we used an temperature increment of 50 K. A smaller increment was used for temperature above 700 K. At each temperature, about 2000 time steps of simulation are performed with the temperature of the system being fixed, which is followed by a few thousand time steps of free run during which the system is allowed to evolve itself without external control. The behaviour of the system is monitored and the temperature is raised only when the system reaches its equilibrium state which is characterized by relatively stable temperature and total-energy values. Thermal expansion is introduced to the TBMD simulation by scaling the lattice parameter according to the empirical formula obtained by Okada and Tokumaru [35], which gives the lattice constant of high-purity silicon as a function of temperature between 300 and 1500 K. For temperatures below 300 K and above 1500 K, the empirical formula by Okada and Tokumaru is extrapolated to obtain an estimate of the lattice constant.

3. Results

The simulation is carried out at temperatures up to 1600 K. Various physical quantities of the system are monitored throughout the simulation at elevated temperatures. It is noted that the lattice parameter of Si at high temperature is almost a linear function of temperature, with a thermal expansion coefficient close to 3.725×10^{-6} (K^{-1}). In figure 2, the height of the topmost surface atom, z_{max}, relative to the bottom fixed layer and the 'volume' of the simulation cell are shown as functions of temperature. Since atoms in the bottom layer are fixed, the height of the topmost surface atom is an indication of the thickness of the simulation slab and is thus referred to as the the 'thickness of the simulation cell' in the following. The volume of the simulation cell is given by $V = (x_{max} - x_{min})(y_{max} - y_{min})z_{max}$, where x_{min} and x_{max} are the x-coordinates of the left- and right-most atoms respectively in the $(33\bar{2})$ direction and y_{min} and y_{max} are the y-coordinates of the similar two atoms at the two extremes in the $(\bar{1}10)$ direction of the simulation cell. The volume of the simulation cell increases smoothly for temperatures up to about 1300 K. On the other hand, the thickness of the simulation slab fluctuates, particularly at high temperature. Nevertheless, a general slow increasing trend for the thickness of the simulation slab as a function of temperature can be observed up to 1300 K. Near 1400 K, the thickness of the simulation slab drops rapidly. In figure 3, the total number of nearest-neighbour bonds in the simulation cell is shown as a function of temperature. Here the number of bonds in the simulation cell increases slowly until about 1400 K above which the number of bonds increases sharply.

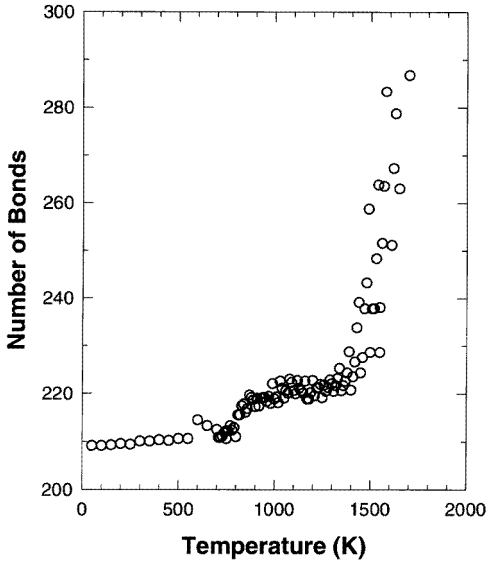

Figure 3. The total number of bonds in the simulation cell is shown as a function of temperature.

In order to analyse the melting behaviour of the Si(113) surface, we calculate the mean square atomic displacement (MSAD) and the static structure factor, $S(\boldsymbol{k})$. The latter is measured in a single-scattering diffraction experiment and is defined as [36]

$$S(\boldsymbol{k}) = \left\langle \left| \sum_{r} n(\boldsymbol{r})\, \mathrm{e}^{\mathrm{i}\boldsymbol{k}\cdot\boldsymbol{r}} \right|^2 \right\rangle$$

where $\boldsymbol{r}$ is the possible position of an atom, $n(\boldsymbol{r})(= 0, 1)$ is the occupancy of electrons and $\langle \cdots \rangle$ denotes the ensemble average. The layer-resolved MSADs obtained in our simulation are shown in figure 4. where the MSAD is averaged over all atoms for each of the upper four layers respectively. As the temperature is raised, the MSAD increases as expected. The MSAD of the surface layer is much larger than those for layers below due to large atomic movements in the surface layer at a given temperature. It becomes smaller for layers further away from the surface.

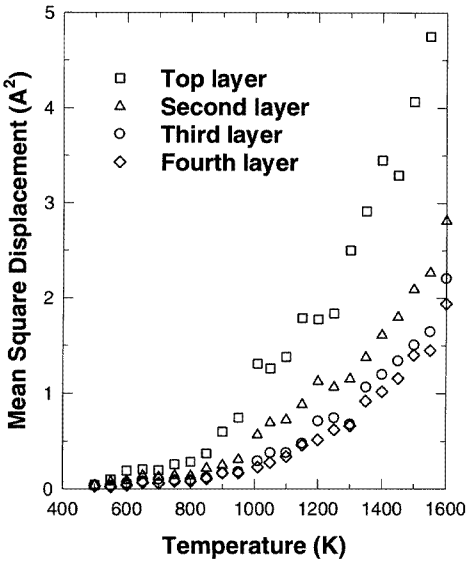

Figure 4. The mean square atomic displacements (MSADs) of the top four layers are shown as functions of temperature.

In figures 5(a) and (b), the MSADs along the three orthogonal directions: $(33\bar{2})$ (x-direction), $(\bar{1}10)$ (y-direction) and (113) (z-direction) are shown for the surface and the next layer, respectively. The atoms in the surface layer have a much larger MSAD in the (113) direction, which is along the normal direction of the surface, than in a direction parallel to the surface. This is expected since a surface atom experiences about half the restoring force of a bulk atom. Typically, experiments show that the thermal excursion of surface atoms perpendicular to the surface is 50–100% greater than a bulk atom at the same temperature. The MSAD obtained in our simulation is in agreement with this observation. It is interesting to note that the MSAD is larger in the $(33\bar{2})$ direction than in the $(\bar{1}10)$ direction. The MSADs in the third and fourth layers (not shown here) are much smaller and become more isotropic which is consistent with the isotropic expansion behaviour of bulk Si.

The static structure factor resembles the essential features of LEED and x-ray experiments. In our TBMD study, the static structure factors are calculated around various low-temperature 3×1 LEED spots in the $\boldsymbol{k}$-space based on the 20 Si atoms in the surface layer. The obtained structure factors at various 3×1 LEED spots show essentially the same feature and temperature dependence. In figure 6(a), the peak value ('diffraction intensity') of the structure factor near the (11) spot is shown as a function of temperature. The corresponding integrated 'intensity' is obtained by numerically integrating the structure

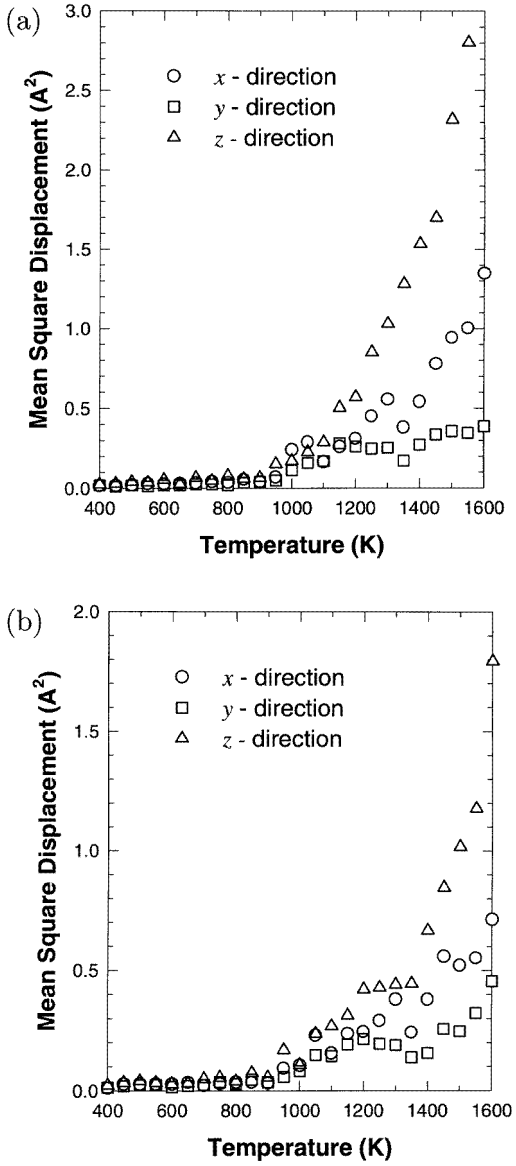

Figure 5. Mean square atomic displacements in the $(33\bar{2})$ (x-) direction (○), the $(\bar{1}10)$ (y-) direction (□) and the (113) (z-) direction (△) are shown as function of temperature for the first layer (a) and the second layer (b), respectively.

factor over $\boldsymbol{k}$ around the spot and is shown in figure 6(b). As temperature increases, the 'intensity' decreases and a sharp drop in the diffracted intensity between 900 K and 1000 K is clearly observable. In order to study the details of the surface disorder, we also calculate the static structure factors along the $(33\bar{2})$ and the $(\bar{1}10)$ directions and the structure factors due to atomic contributions from the other layers. In figure 7, the static structure factors along the $(33\bar{2})$ and the $(\bar{1}10)$ directions are presented as functions of temperature. It is clear from the figure that the disordering of the surface layer is asymmetric and the static

structure factor in the $(33\bar{2})$ direction is much smaller than in the $(\bar{1}10)$ direction, indicating much larger atomic motions in the $(33\bar{2})$ direction than in the $(\bar{1}10)$ direction. In figure 8, the static structure factor of the surface layer is compared with those of the next three layers. As expected, the structure factor of the surface layer is much smaller than those of the inner layers. The structure factors of the inner layers also show a layer by layer decrease, even though they are very close. From figure 8, we also note that the structure factors of the inner layers show very small change for temperature up to 1300 K. Significant drops in these structure factors occur only at temperature above 1300 K.

Another indicator for crystal melting is the time development of the mean square displacement, defined by

$$\Delta \boldsymbol{r}^2(t) = \frac{1}{N}\sum_{i=1}^{N} |\boldsymbol{r}_i(t) - \boldsymbol{r}_i(0)|^2.$$

For a solid, $\Delta \boldsymbol{r}^2(t)$ remains nearly constant, while for a fluid it increases almost linearly with time. The time derivative of the mean square displacement is proportional to the self-diffusion coefficient D. We have calculated the 2D self-diffusion coefficient (assuming $\boldsymbol{r}$ to be a 2D vector in the surface plane) for atoms in the surface layer at each elevated temperature and the results are shown in figure 9. Clear increases of the diffusion coefficient can be seen around 900 K and 1400 K.

4. Discussion

From the simulated results shown in figures 2–8, various physical quantities of the system exhibit normal crystalline behaviours for temperatures up to 800 K. The thickness and volume of the simulation cell, total number of bonds in the simulation cell, the mean square atomic displacements, and the structure factors either change smoothly or remain roughly constants as functions of temperature. These indicate that the surface behaves as a solid surface in this temperature range. As temperature increases, the vibration amplitudes of atoms in the surface layer become larger as indicated by the increased MSADs. However, the surface remains commensurate as the static structure factor is about the same throughout this temperature range.

Above 800 K, the system begins to show some abnormal behaviour. In figure 2, we can see that the fluctuation in thickness of the simulation slab becomes more evident. A jump in the total number of bonds in the simulation cell can also be seen in figure 3 above 800 K, which is a clear indication of a phase transition. The MSAD in the surface layer also increases much faster and a clear increase in the 2D self-diffusion coefficient is shown around 900 K in figure 9. A sharp decrease in the static structure factor can be seen around 950 K in figure 6 for the (11) spot. Similar trends can also be seen for other 3×1 diffraction spots. All these indicate that a phase transition takes place in the 2D surface layer. Judging from the relatively small static structure factor for $T > 1000$ K, the surface is significantly disordered and is in an incommensurate, quasi-liquid state. However, it is not completely disordered. The underlying ordered layers may induce some residual short-range order which results in a non-zero structure factor in this temperature range. Due to the fact that the transition is very broad, the exact transition temperature cannot be determined from the graphs shown here. However, if we take the inflection point in the 'integrated intensity' as an estimate, the transition temperature should be around 950 K, which coincides with the transition temperature observed experimentally [16–19].

From LEED and x-ray experiments [16–19], an order–disorder (i.e. commensurate–

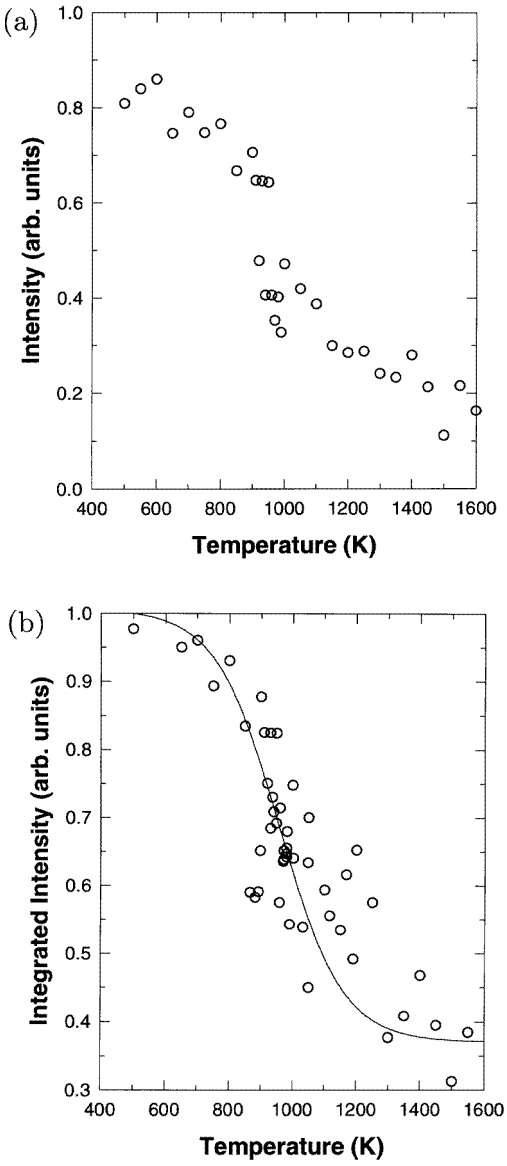

Figure 6. The maximum of structure factor ('diffraction intensity') (a) and the integrated intensity (b) of the (11) spot are shown as functions of temperature. The solid line is a guide to the eye.

incommensurate) phase transition is observed at 950 K. In both types of experiments the peak intensity decreases drastically and shifts in the $(1\bar{1}0)$ direction at the critical temperature. Furthermore, intensity profiles of the various spots also indicate an asymmetric broadening parallel and perpendicular to the $(1\bar{1}0)$ direction, which reflects the different behaviours of the corresponding correlation lengths. The broader shapes parallel to the $(1\bar{1}0)$ direction reflect smaller correlation length in that direction. This observed shift of the LEED spots to smaller momentum values was attributed to the presence of domain walls. In our TBMD

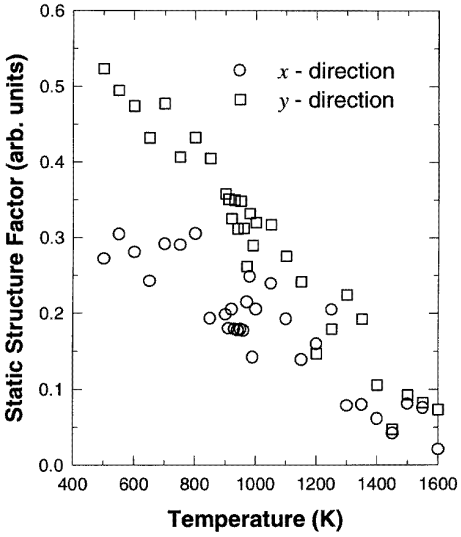

Figure 7. Structure factors along the $(33\bar{2})$ (x-) direction (○) and the $(\bar{1}10)$ (y-) direction (□) are shown as functions of temperature.

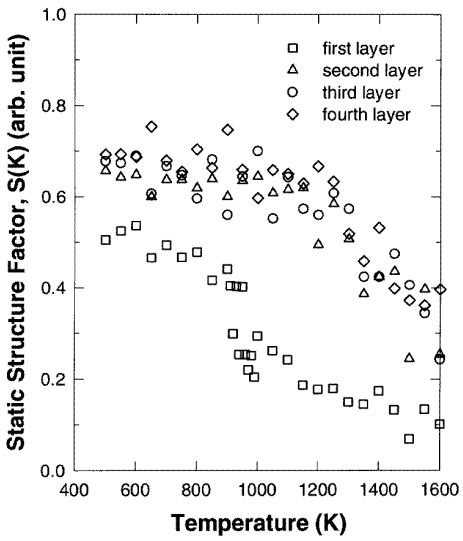

Figure 8. Structure factors of the top four layers are shown as functions of temperature.

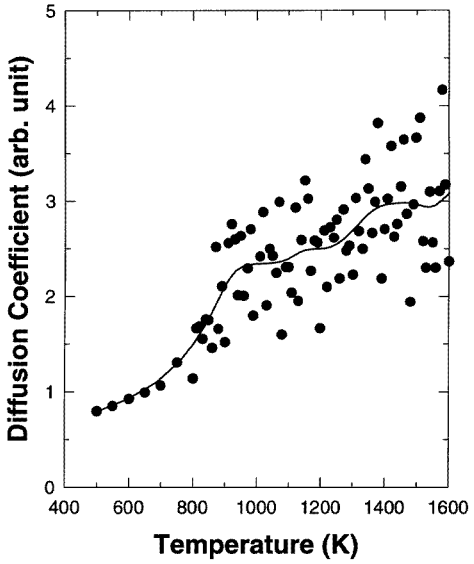

Figure 9. The 2D self-diffusion coefficient is shown as a function of temperature. The solid line is a Bazier curve fitted to the data points.

simulation, we have simulated what might be observed in the LEED and x-ray experiments by computing the structure factor. The structure factor does show a sharp decrease around 950 K, in agreement with observations in LEED and x-ray experiments. Unfortunately due to the fact that the simulation cell is only one unit wide in the $(\bar{1}10)$ direction, the shifting and broadening of the diffraction peaks are not clearly seen in our simulation. Therefore,

we cannot compare our simulated melting of the Si(113) surface to chiral melting. Further simulation with a larger simulation cell might reveal features related to chiral melting and help to determine whether the simulated melting of the Si(113) surface satisfies the criterion for chiral melting. On the other hand, the simulated MSAD and static structure factor shown in figures 5 and 7 respectively do show some anisotropic nature in the surface layer. A larger MSAD and a smaller diffraction intensity are observed in the $(33\bar{2})$ direction than in the $(\bar{1}10)$ direction, which suggests that the correlation length in the $(33\bar{2})$ direction is smaller than that in the $(\bar{1}10)$ direction. This, however, contradicts the observations in LEED and x-ray experiments mentioned above where correlation length in the $(\bar{1}10)$ direction is found to be smaller. This again might be attributed to the small simulation cell which might confine the motion of surface atoms in the $(\bar{1}10)$ direction.

The surface remains in the incommensurate, quasi-liquid state for temperatures up to 1300 K. As can be seen in figure 8, the surface layer is significantly disordered while the underneath layers are still in a crystalline solid structure as indicated by the fairly constant structure factors in this temperature range. Detailed examination of the atomic trajectories shows large incoherent atomic displacements in the surface layer while the second layer still remains ordered in this temperature range.

At temperatures above 1300 K, the system undergoes some drastic changes. First we notice in figure 2 that the thickness of the simulation slab drops quickly. Meanwhile the total number of bonds in the simulation cell increases rapidly (figure 3). Furthermore, the static structure factors of the atomic layers below the surface start to decrease as shown in figure 8. The 2D self-diffusion coefficient is further increased due to disordering in the atomic layers below the surface layer. Snapshots of atomic trajectories show that some of the surface atoms diffuse into the second layer and the layer structure is no longer observable for atoms which were in the top two layers. All these may be considered as evidence for surface-induced crystal melting.

From experimental observations [37, 38], the structural property of Si on melting is such that there is a contraction of the loose-packed diamond structure which is of the order of 10%. In our study, due to the assumption of bulk thermal expansion throughout the simulation in the lateral directions, which leads to an approximate quadratic increase of the surface area as a function of temperature, the volume of the simulation cell increases monotonically as temperature is raised. However, the rapid decrease of the slab thickness around 1400 K is clearly reflected in the volume of the simulation cell as the rate of volume increase is reduced around 1400 K. Furthermore, it has been shown that the coordination number changes during melting from four in the diamond structure to 6.5 in the liquid state, with a substantial increase in the bond length, from 2.35 to 2.5 Å. The increase in the total number of bonds in the simulation cell agrees qualitatively with this prediction.

A simple estimate of the melting temperature comes from the Lindemann criterion which states that the crystal melts when the mean square atomic displacement due to thermal vibrations, $\langle \boldsymbol{r}^2 \rangle$, is a significant fraction ($\sim$25%) of the lattice constant [39]. It can be seen in figure 4 that the Lindemann criterion is well satisfied here since the MSAD of the second layer at 1400 K becomes larger than 1.5 Å^2 which is larger than 25% of the lattice constant in bulk Si. We therefore conclude that the disordering of the surface layer causes disordering of the second layer at approximately 1400 K and eventually leads to melting of the crystal at a slightly higher temperature.

The MSAD in the surface layer is the largest and for layers below the MSAD becomes smaller and smaller. This seems to suggest that the crystal should melt in a layer by layer fashion [39]: each layer melts when it becomes significantly disordered and its local Lindemann condition is met and, therefore, the melt front propagates into the crystal with

increasing temperature until the process is finally completed. This is likely to happen as a disordered layer at the surface exerts a perpendicular restoring force on a second-layer atom that is intermediate between that of an ordered surface layer and the vacuum. Accordingly, the second layer melts at a slightly higher temperature than the surface but still lower than the bulk value. A similar argument applies to the third layer, and so on. Other mechanisms of surface melting have been proposed based on classical molecular-dynamics simulation. For example, study of the Si(100) surface using the Stillinger–Weber potential has shown that melting proceeds via diffusive motion in close-packed facets [40]. Our present study is limited to the solid phase; even when there are indications that surface melting is about to occur, it is impossible to simulate the complete solid–liquid transition of the system. Further study is required to investigate the melting process of the Si(113) surface and to determine the exact melting temperature. However, as a rough estimate, the crystal should melt at a temperature which is slightly higher than 1400 K but lower than the bulk melting temperature of 1685 K [41] based on the facts that the second layer becomes disordered at 1400 K and the structure factors of the layers below are close to that of the second layer. Since the melting is initiated by surface disordering, it is expected that the melting temperature is lower than that of the bulk.

5. Conclusion

Using the TBMD simulation method, we are able to observe an order–disorder phase transition of the Si(113) surface near 950 K. The behaviours of most of the observed quantities, including the MSAD and the structure factor, as temperature increases indicate that the surface layer begins to disorder at about 950 K which coincides with the order–disorder transition temperature observed in chiral melting. Even though further work is required to confirm whether the observed phase transition complies with chiral melting, the simulation did show certain features that have been observed in experiments, such as the anistropic disordering of the surface layer. The surface is predicted to be in an incommensurate, quasi-liquid state where the surface layer disorders significantly while the underneath layers remain commensurate between 1000 K and 1400 K. The disordering of the surface layer induces disordering in the second layer at about 1400 K which further initiates disordering in the inner layers and leads to melting of the crystal.

Despite various limitations such as the small simulation cell, relatively short simulation time and finite temperature increments in this preliminary study, it is encouraging to be able to observe the various indications for surface disordering and melting. The complete melting process may be studied with a larger simulation cell, longer simulation time and more consistent treatment of thermal expansion.

References

[1] Chadi D J 1984 *Phys. Rev.* B **29** 785
[2] Heckingbottom R and Wood P R 1970 *Surf. Sci.* **23** 437
[3] Olshanetsky B Z and Mashanov V I 1981 *Surf. Sci.* **111** 414
[4] Myler U and Jacobi K 1989 *Surf. Sci.* **220** 353
[5] Knall J, Pethica J B, Todd J D and Wilson J H 1991 *Phys. Rev. Lett.* **66** 1733
[6] Wilson J H, Scott P D, Pethica J B and Knall J 1991 *J. Phys.: Condens. Matter* **3** 133
[7] Althainz P, Myler U and Jacobi K 1990 *Phys. Rev.* B **41** 2849
[8] Jacobi K, Myler U and Althainz P 1990 *Phys. Rev.* B **41** 10 721
[9] Althainz P, Myler U and Jacobi K 1991 *Phys. Rev.* B **43** 14 157
[10] Myler U, Althainz P and Jacobi K 1991 *Surf. Sci.* **251–252** 607

[11] Jacobi K and Myler U 1993 *Surf. Sci.* **284** 223
[12] Dabrowski J, Müssig H J and Wolff G 1994 *Phys. Rev. Lett.* **73** 1660
[13] Scholz S M and Jacobi K 1995 *Phys. Rev.* B **52** 5795
[14] Xing Y R, Zhang J P, Wu J A, Liu C Z and Wang C H 1990 *Surf. Sci. Lett.* **232** L215
[15] Feng Y P, Wee T H, Ong C K and Poon H C 1996 *Phys. Rev.* to appear
[16] Schreiner J, Jacobi K and Selke W 1994 *Phys. Rev.* B **49** 2706
[17] Abernathy D L, Birgeneau R J, Blum K I and Mochrie S G J 1993 *Phys. Rev. Lett.* **71** 750
[18] Abernathy D L, Song S, Blum K I, Birgeneau R J and Mochrie S G J 1994 *Phys. Rev.* B **49** 2691
[19] Yang Y-N, Williams E D, Park R L, Bartelt N C and Einstein T L 1990 *Phys. Rev. Lett.* **64** 2410
[20] Ranke W 1990 *Phys. Rev.* B **41** 5243
[21] Wilson J H, McInnes D A, Knall J, Sutton A P and Pethica J B 1992 *Ultramicroscopy* **42–44** 801
[22] Hadley M J, Tear S P, Röttger B and Neddermeyer H 1993 *Surf. Sci.* **258** 280
[23] Bird D M, Clarke L J, King-Smith R D, Payne M C, Stick I and Sutton A P 1992 *Phys. Rev. Lett.* **69** 3785
[24] Huang H, Tong S Y, Myler U and Jacobi K 1994 *Surf. Rev. Lett.* **1** 221
[25] Jacobi K, Gruyters M, Geng P, Bitzer T, Aggour M, Rauscher S and Lewerenz H-J 1995 *Phys. Rev.* B **51** 5437
[26] Khan F S and Broughton J Q 1989 *Phys. Rev.* B **39** 3688
[27] Wang C Z, Chan C T and Ho K M 1989 *Phys. Rev.* B **39** 8592
[28] Goodwin L, Skinner A J and Pettifor D G 1989 *Europhys. Lett.* **9** 701
[29] Laasonen K and Nieminen R M 1990 *J. Phys.: Condens. Matter* **2** 1509
[30] Lim H S, Low K C and Ong C K 1993 *Phys. Rev.* B **48** 1595
[31] Low K C and Ong C K 1994 *Phys. Rev.* B **50** 5352
[32] Low K C, Lim H S and Ong C K 1994 *J. Phys.: Condens. Matter* **6** 9551
[33] Tománek D and Schlüter M A 1986 *Phys. Rev. Lett.* **56** 1055; 1987 *Phys. Rev.* B **36** 1208
Alerhand O L and Mele E J 1987 *Phys. Rev.* B **35** 5533
[34] Ryckaert J P, Ciccotti G and Berendsen H J C 1977 *J. Comput. Phys.* **23** 327
[35] Okada Y and Tokumaru Y 1984 *J. Appl. Phys.* **56** 314
[36] Bartelt N C, Einstein T L and Roelofs L D 1987 *Phys. Rev.* B **35** 4812
[37] Gabathuler J P and Steeb S 1979 *Z. Naturf.* a **34** 1614
[38] Gaspard J P, Lambin Ph, Mouttet C and Vigneron J P 1984 *Phil. Mag.* B **50** 103
[39] Zangwill A 1988 *Physics at Surfaces* (Cambridge: Cambridge University Press)
[40] Lampinen J, Nieminen R M and Kaski K 1988 *Surf. Sci.* **200** 101
[41] Hultgren R, Desai P D, Hawkins D T, Gleiser M, Kelly K K and Wagman D D 1973 *The Thermodynamic Properties of the Elements* (Metals Park, OH: American Society for Metals)